

## Research Paper

# Tumor Characterization with Dynamic Contrast Enhanced Magnetic Resonance Imaging and Biodegradable Macromolecular Contrast Agents in Mice

Xueming Wu,<sup>1</sup> Yi Feng,<sup>2</sup> Eun-Kee Jeong,<sup>3</sup> Lyska Emerson,<sup>4</sup> and Zheng-Rong Lu<sup>1,5,6</sup>

Received March 23, 2009; accepted June 29, 2009; published online July 14, 2009

**Purpose.** To investigate the efficacy of polydisulfide-based biodegradable macromolecular contrast agents of different degradability and molecular weight for tumor characterization based on angiogenesis using dynamic contrast enhanced MRI (DCE-MRI).

**Methods.** Biodegradable macromolecular MRI contrast agents, Gd-DTPA cystamine copolymers (GDCC) and Gd-DTPA cystine copolymers (GDCP), with molecular weight of 20 and 70 kDa were evaluated for tumor characterization. Gd(DTPA-BMA) and a prototype of macromolecular contrast agent, albumin-(Gd-DTPA), were used as controls. The DCE-MRI studies were performed in nude mice bearing MDA PCa 2b and PC-3 human prostate tumor xenografts. Tumor angiogenic kinetic parameters including endothelium transfer coefficient ( $K^{\text{trans}}$ ) and fractional tumor plasma volume ( $f^{\text{PV}}$ ) were calculated from the DCE-MRI data using a two-compartment model and compared between the two different tumor models for each contrast agent.

**Results.** There was no significant difference in the  $f^{\text{PV}}$  values between two tumor models estimated with the same agent except for GDCC-70. The  $K^{\text{trans}}$  values in both tumor models decreased with the increase of molecular weight of contrast agents. With the same high molecular weight (70 kDa), GDCC-70 showed a higher  $K^{\text{trans}}$  values than GDCP-70 due to high degradability of the former in both tumor models ( $p < 0.05$ ). The  $K^{\text{trans}}$  values of MDA PCa 2b tumors were significantly higher than those of PC-3 tumors estimated by Gd(DTPA-BMA), GDCC-20, GDCC-70, GDCP-70, and albumin-(Gd-DTPA) ( $p < 0.05$ ).

**Conclusions.** The polydisulfide-based biodegradable macromolecular MRI contrast agents are promising in tumor characterization and differentiation with dynamic contrast enhanced MRI.

**KEY WORDS:** biodegradable macromolecular contrast agent; dynamic contrast enhanced MRI; polydisulfides; tumor characterization.

## INTRODUCTION

Accurate tumor characterization is critical for cancer patient care management. For example, more than 30% of men older than 50 years have microscopic prostatic carcinoma at autopsy; fewer than 10% of them finally develop malignant prostate cancer (1,2) and therefore need aggressive treatment (3). Thus, accurate and reliable non-invasive

methods are needed to characterize different tumors and define the malignancy of every individual carcinoma. Tumor angiogenesis has been considered as a valuable parameter for tumor characterization, and it is directly associated with tumor malignancy and metastasis. Tumor angiogenesis can be correlated to tumor vascularity, which is determined by intratumoral vascular permeability and microvessel density (MVD) (4–7). High vessel densities, proliferation of endothelial cells and increased vascular permeability in tumors often result in tumor aggression and poor prognosis (8,9). Dynamic contrast enhanced MRI (DCE-MRI) is a non-invasive imaging modality, which has become an important tool in cancer diagnosis, differentiating benign from malignant lesions and monitoring antiangiogenic therapy (8,10). DCE-MRI acquires MR images repetitively and can provide quantitative measurement of tumor vascular parameters, such as endothelial transfer coefficient ( $K^{\text{trans}}$ ) and fractional tumor plasma volume ( $f^{\text{PV}}$ ) (11,12). These quantitative parameters can be correlated to tumor vascularity and angiogenesis, and can be used for assessing the efficacy of anticancer therapies, including antiangiogenic therapy (2,13).

It has been reported that the molecular weight or particle size of MRI contrast agents has a significant impact on tumor

Xueming Wu and Yi Feng made equal contribution in this work.

<sup>1</sup> Department of Pharmaceutics and Pharmaceutical Chemistry, University of Utah, Salt Lake City, Utah, USA.

<sup>2</sup> Department of Materials Science and Engineering, University of Utah, Salt Lake City, Utah, USA.

<sup>3</sup> Department of Radiology, University of Utah, Salt Lake City, Utah, USA.

<sup>4</sup> Department of Pathology, University of Utah, Salt Lake City, Utah, USA.

<sup>5</sup> Department of Biomedical Engineering, Case Western Reserve University, Wickenden 427, 10900 Euclid Avenue, Cleveland, Ohio 44106-7207, USA.

<sup>6</sup> To whom correspondence should be addressed. (e-mail: zxl125@case.edu)

vascular parameters determined by DCE MRI (11,14,15). MRI contrast agents with different sizes have been investigated for tumor differentiation based on tumor angiogenesis and vascular permeability. Low molecular weight Gd(III)-based contrast agents often overestimate tumor blood volume and vascular permeability because these agents rapidly extravasate from the blood to the extracellular space in tumor tissue (16–18). Macromolecular contrast agents have shown better assessment in tumor angiogenesis than low molecular weight contrast agents (19,20). For example, albumin-(Gd-DTPA), a prototype macromolecular MRI contrast agent, was able to differentiate tumor vascular permeability and provided more accurate tumor characterization than the low molecular weight contrast agents (21,22). Good correlation has also been reported between the histological analysis and tumor vascular permeability estimated by DCE-MRI and macromolecular contrast agent, but not for low molecular weight agents (11). However, macromolecular MRI contrast agents are not available for clinical applications because of the safety concerns related to their slow excretion and high tissue accumulation of toxic Gd(III) ions (20,23).

We have recently developed polydisulfide Gd(III) chelates as biodegradable macromolecular MRI contrast agents to facilitate the excretion of Gd(III) chelates after the MRI examinations. These agents initially behave as macromolecular agents and result in superior contrast enhancement in the vasculature and tumor tissues. They can then be degraded *in vivo* into oligomeric and low molecular weight Gd(III) chelates, which rapidly excrete from the body through renal filtration, resulting in minimal tissue accumulation (24,25), similar to that of low molecular weight contrast agents (23,26,27). The biodegradable macromolecular MRI contrast agents are also effective for evaluation of tumor angiogenesis and vascular permeability with DCE-MRI (28). The purpose of this study was to evaluate the efficacy of the polydisulfide Gd(III) complexes in tumor differentiation with DCE-MRI. Tumor vascular parameters derived from the DCE-MRI data were compared in mice bearing PC-3 and MDA PCa 2b human prostate cancer xenografts.

## MATERIALS AND METHODS

### Contrast Agents

Gd(DTPA-BMA) (Omniscan®, 574 Da) was obtained from Nycomed Inc., Princeton, NJ. Gd-DTPA cystamine copolymers (GDCC) and Gd-DTPA cystine copolymers (GDCCP) were prepared as previously described (25,26). GDCCP are modified polydisulfide Gd(III) complexes with slower degradation rates than GDCC. They were further fractionated using a Sephacryl S-300 column on a Pharmacia FPLC system (Gaithersburg, MD) to prepare the agents with narrow molecular weight distributions. The apparent molecular weights of the fractions were determined by size exclusion chromatography using poly[N-(2-hydroxypropyl) methacrylamide] as a standard on an AKTA FPLC system (GE Biosciences, Piscataway, NJ). Albumin-(Gd-DTPA) (92 KDa) was prepared as previously described (29). The Gd(III) content in the agents was determined by inductively

coupled plasma optical emission spectroscopy (ICP-OES, Perkin Elmer Optima 3100XL).

### Tumor Cells and Animal Models

Human prostate cancer MDA PCa 2b and PC-3 cell lines were obtained from American Type Culture Collection (ATCC, Manassas, VA) with ATCC numbers CRL-2422 and CRL-1435, respectively. PC-3 cell line was cultured using ATCC complete growth medium (F-12K medium with 10% fetal bovine serum). MDA PCa 2b cell line was cultured with Kaighns modification of Hams F12 medium (F12K) with 2 mM L-glutamine and 1.5 g/L sodium bicarbonate, supplemented with 25 ng/ml cholera toxin, 10 ng/ml epidermal growth factor, 0.005 mM phosphoethanolamine, 100 pg/ml hydrocortisone, 45 nM selenious acid, 0.005 mg/ml insulin, and 20% fetal bovine serum according to ATCC's instruction. The MDA PCa 2b cells grew in clumps, formed layers, and had a doubling time of 14 days with great tumorigenicity (30). PC-3 cells had a tumor doubling time of 8.5 days.

Athymic male NCr-nu/nu nude mice at 5 weeks old were purchased from National Cancer Institute at Frederick, MD. Cell suspension of MDA PCa 2b or PC-3 in their preferred medium was mixed with Matrigel matrix (BD Biosciences, San Jose, CA) at a 1:1 ratio.  $5 \times 10^6$  cells in 120  $\mu$ L mixture were inoculated subcutaneously in both right and left sides of the mouse's hip. DCE-MRI study was performed when the tumors reached about 1 cm in diameter (14 weeks after MDA PCa 2b cell inoculation, 4 weeks after PC-3 inoculation) (31–34).

### Dynamic Contrast-Enhanced MRI (DCE-MRI)

All images were acquired on a Siemens Trio 3T scanner using the system body coil for RF excitation and a human wrist coil for RF reception. A group of three mice weighing 28 g were used for each agent. Mice were anesthetized with an intraperitoneal injection of a mixture of ketamine (Bedford, OH, 90 mg/kg) and xylazine (St. Joseph, MO, 10 mg/kg). They were then placed prone with the tumors located at the center of a human wrist coil. A tail vein was catheterized using a 30 gauge needle connected to a 2-m long thin tubing filled with heparinized saline. 120  $\mu$ L of contrast agent was injected via the tubing, and 200  $\mu$ L saline was used to flush the tubing after the injection of contrast agent. The dose for all contrast agents was 0.1 mmol-Gd/kg except that the dose for albumin-(Gd-DTPA) was 0.03 mmol-Gd/kg as reported in literatures.

Before the injection, 3D fast low angle shot (FLASH) images and 2D axial spin echo (SE) images were acquired. The 3D FLASH image was used to define the regions of interest (ROIs) for 2D SE image. The axial slices in 2D SE images were selected for the acquisition of DCE-MRI data. Dynamic MRI scan was performed using 2D FLASH for a period of 15 min. After a 45 s delay, the contrast agent was administered via the tubing. 2D axial SE scans were acquired at 15 min after the injection. Parameters of the 3D FLASH pulse sequence are: TR/TE=7.75/2.56 ms,  $\alpha=25^\circ$ , 0.5 mm coronal slice thickness, averages of 4, fat saturation, and 81 sec scan time. Parameters of the 2D SE pulse sequence are TR/TE=400/10 ms,  $\alpha=90^\circ$ , 2 mm axial slice thickness, averages of 2, fat saturation, eight slices and 61 sec scan time.

Parameters of the 2D FLASH pulse sequence (for dynamic scans) are TR/TE=104/4.46 ms,  $0.5 \times 0.5 \times 1.5$  mm,  $\alpha=30^\circ$ , 1.5 mm axial slice thickness, single acquisition, a total of 10 axial slices (covering majority of the tumor with the last two slices cover the heart), and 11 s scan time for a single acquisition.

### Data Analysis

The 3D FLASH and 2D SE images were reconstructed and analyzed using Osirix (<http://homepage.mac.com/rossetantoine/osirix/>). A package of programs based on MATLAB (The MathWorks, Inc., Natick, MA) was developed to process dynamic 2D FLASH data in DICOM format. Regions of interest (ROIs) were placed in the whole tumor and in the right ventricle of the heart to obtain signal intensity (SI) in the blood. The average MR signal intensity of the ROIs before the ( $SI_{pre}$ ) contrast agent injection was used as the baseline and was subtracted from the SI after contrast agent injection ( $SI_{post}$ ) to calculate the increase in SI ( $\Delta SI$ ). It is assumed that  $\Delta SI$  is proportional to the change of the contrast agent concentration, which is a reasonable approximation at low contrast agent concentration (35). The signal-time kinetic data were analyzed using a two-compartment bidirectional exchange kinetic model as shown in the equation

$$C_T(t) = K^{trans} \int_0^t C_p(\theta) e^{-k_{ep}(t-\theta)} d\theta + f^{PV} C_p(t),$$

where  $C_p$  and  $C_T$  are the contrast agent concentrations in blood and tumor, respectively;  $K^{trans}$  is the endothelial transfer coefficient;  $k_{ep}$  is the rate constant of reflux from the extravascular and extracellular space (EES) back to blood. The tumor endothelial transfer coefficient ( $K^{trans}$ ) and fractional tumor plasma volume ( $f^{PV}$ ) were similarly calculated by the methods as described in the literature (11).

### Histological Study

The mice were sacrificed at the end of the experiments. Tumors were collected and fixed in 10% buffered formalin and embedded in paraffin. Tissue sections were cut at  $4\mu\text{m}$  and prepared on uncharged slides. Some of the tissue sections were stained with hematoxylin and eosin and analyzed by microscopy. The rest of tissue section was immunostained with rabbit polyclonal antibodies to factor VIII antigen. Histological analysis of microvessel density count was performed as described in the literature (36).

### Statistical Analysis

Statistical analysis was performed using a student t-test (GraphPad Prism; GraphPad Software, San Diego, CA). P values were two-tailed with a confidence interval of 95%.

## RESULTS

### Contrast Agents

The polydisulfide Gd(III) complexes, GDCC and GDGP, with narrow molecular weight distributions and different

molecular weights were prepared by fractionation of the polydisulfides with size exclusion chromatography. Table I lists the number averaged molecular weight ( $M_n$ ), weight averaged molecular weight ( $M_w$ ), polydispersion index (PDI), and  $T_1$  relaxivity per complexed Gd(III) ion at 3T of the polymeric contrast agents. The agents with molecular weights of 20 and 70 KDa, GDCC-20, GDCC-70, GDGP-20 and GDGP-70, were chosen to represent low and high molecular weight contrast agents. The apparent weight and number averaged molecular weights of a control macromolecular contrast agent, albumin-(Gd-DTPA), were 44 and 45 KDa, respectively, relative to the linear poly[N-(2-hydroxypropyl) methacrylamide] standards.

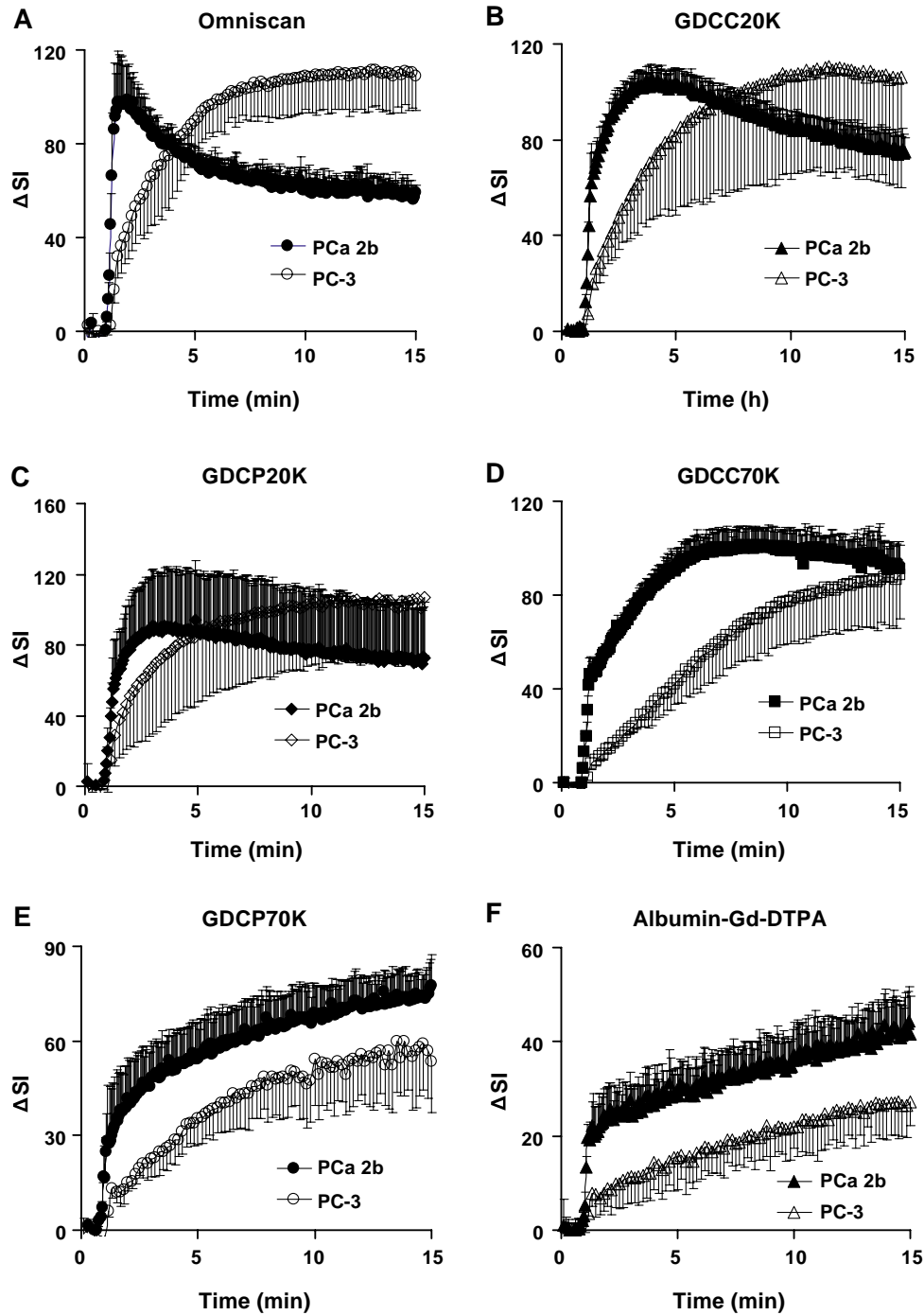
### Dynamic Contrast-Enhanced MRI (DCE-MRI)

Figure 1 shows the representative MR signal intensity-time course in both PC-3 and MDA PCa 2b tumor tissues for each contrast agent. Since the endothelial transfer coefficient ( $K^{trans}$ ) measures the perfusion of the contrast agents from the blood circulation into tumor extracellular space, and the fractional tumor plasma volume ( $f^{PV}$ ) is associated to the initial SI rise in tumor tissue, the DCE-MRI study was focused on the contrast uptake kinetics in the first 15 min after the injection. The tumor uptake kinetics varied with the tumor tissues and properties of the contrast agents. After the initial SI rise, the diffusion of contrast agents into the extracellular space was controlled by the contrast agent concentration in the blood and the permeability of the tumor microvessels. The MDA-PCa-2b tumor exhibited more rapid uptake kinetics than the PC-3 tumor for all tested contrast agents. For the same tumor, contrast uptake kinetics slowed down with the increasing molecular weight and decreasing degradability of the agents. GDGP was less degradable than GDCC and showed slower tumor uptake than GDCC with the same molecular weights. Albumin-(Gd-DTPA) was non-degradable and had much slower tumor uptake kinetics than GDCC and GDGP of both molecular weights in both tumors.

Table II lists the tumor endothelial transfer coefficient ( $K^{trans}$ ) and fractional tumor plasma volume ( $f^{PV}$ ) calculated with the two-compartment model from the DCE-MRI data obtained with the contrast agents in both PC-3 and MDA PCa 2b tumors. The comparison of the vascular parameters estimated for PC-3 and MDA PCa 2b tumors by different contrast agents was shown in Fig. 2. Although MDA PCa 2b tumor has a slower growth rate than PC-3 tumor, the  $K^{trans}$

**Table I.** Physicochemical Properties, Including  $M_n$ ,  $M_w$ , PDI and Relaxivity ( $r_1$ ), of Contrast Agents Used

	$M_n$ , KDa	$M_w$ , KDa	PDI	$r_1$ , $\text{mM}^{-1}\text{s}^{-1}$ (3T)
Gd(DTPA-BMA)	0.574		N/A	4.62
GDCC20K	20	21	1.06	5.45
GDGP20K	19	21	1.07	6.04
GDCC70K	68	73	1.07	5.35
GDGP70K	68	73	1.08	6.44
Albumin-(Gd-DTPA)	44	45	1.02	7.05



**Fig. 1.** Comparison of MR signal intensity ( $\Delta SI$ ) time curves for the whole tumors of PC-3 and MDA PCa 2b xenografts enhanced by Gd(DTPA-BMA), GDCC-20, GDCC-70, GDCC-70, GDCC-70, and albumin-(Gd-DTPA).

values of MDA-PCa-2b tumor were significantly higher than those of PC-3 tumor with similar tumor size estimated by all agents except GDCC-20 ( $p < 0.05$ ). For the same tumor model, the  $K^{\text{trans}}$  value decreased with the increase of molecular weight and decrease of degradability of the contrast agents. The low molecular weight agent Gd(DTPA-BMA) resulted in the highest  $K^{\text{trans}}$  values while the albumin-(Gd-DTPA) gave the lowest  $K^{\text{trans}}$  in both tumor models. The  $K^{\text{trans}}$  values of GDCC-20, GDCC-20, GDCC-70 and GDCC-70 were

between those of Gd(DTPA-BMA) and albumin-(Gd-DTPA). GDCC with a slower degradability resulted in smaller  $K^{\text{trans}}$  values than GDCC with similar molecular weight, except GDCC-20 for PC-3 tumor. There was no significant difference in the values of  $I^{\text{PV}}$  estimated by most of the contrast agents between two tumors. Histological analysis showed that there was no significant difference in the microvessel density between two tumors based on immunostain of factor VIII antigen.

**Table II.** Vascular Parameters  $K^{trans}$  and  $f^{PV}$  of PC-3 and MDA PCa 2b Tumors Estimated by Gd(DTPA-BMA), GDCC-20, GDCC-70, GDCC-20, GDCC-70, GDCC-70 and Albumin-(Gd-DTPA)

	$K^{trans}$		$f^{PV}$	
	PC-3	MDA PCa 2b	PC-3	MDA PCa 2b
Gd-DTPA-BMA	0.130±0.029	0.402±0.025 **	0.088±0.086	0.110±0.058
GDCC20K	0.081±0.021	0.294±0.049 **	0.070±0.032	0.069±0.040
GDCC70K	0.115±0.121	0.189±0.067	0.087±0.077	0.065±0.055
GDCC20K	0.043±0.015	0.075±0.022 *	0.019±0.007	0.099±0.015 **
GDCC70K	0.023±0.008	0.047±0.013 **	0.033±0.025	0.075±0.051
albumin-(Gd-DTPA)	0.005±0.002	0.008±0.002 *	0.045±0.029	0.074±0.016

\* ( $P<0.05$ ), \*\* ( $P<0.01$ ) indicates  $K^{trans}$  or  $f^{PV}$  are significantly different between PC-3 and MDA PCa 2b.

## DISCUSSION

Dynamic contrast enhanced (DCE) MRI non-invasively measures the uptake kinetics of a contrast agent in tumor tissues. The vascular parameters calculated from the uptake kinetics can be used as biomarkers to characterize individual tumors. These biomarkers can be used for non-invasive tumor grade and evaluation of tumor response to anticancer therapies. Low molecular weight contrast agents, which are exclusively used in clinical studies, rapidly extravasate through both tumor blood vessels and normal blood vessels and are not ideal for tumor characterization. Macromolecular contrast agents with molecular weights larger than 20 KDa have limited extravasation through normal blood vessels and can selectively pass through porous tumor blood vessels. They are considered to be effective for more accurate tumor

characterization with DCE-MRI. The use of macromolecular MRI contrast agents has been approved to be successful to monitor the permeability changes of tumor vasculature cause by some cancer therapies including radiation (37), chemo (11), or anti-vascular therapy (10).

Unfortunately, macromolecular contrast agents are not available for clinical application because of safety concerns. Polydisulfide-based biodegradable macromolecular MRI contrast agents have been developed to alleviate the safety concerns (25–27). The biodegradable macromolecular contrast agents can be rapidly excreted from the body after the MRI studies and have showed minimal long-term tissue accumulation comparable to that of low molecular weight clinical contrast agents. These agents have shown promises to be further developed for clinical applications, including tumor characterization with DCE-MRI.

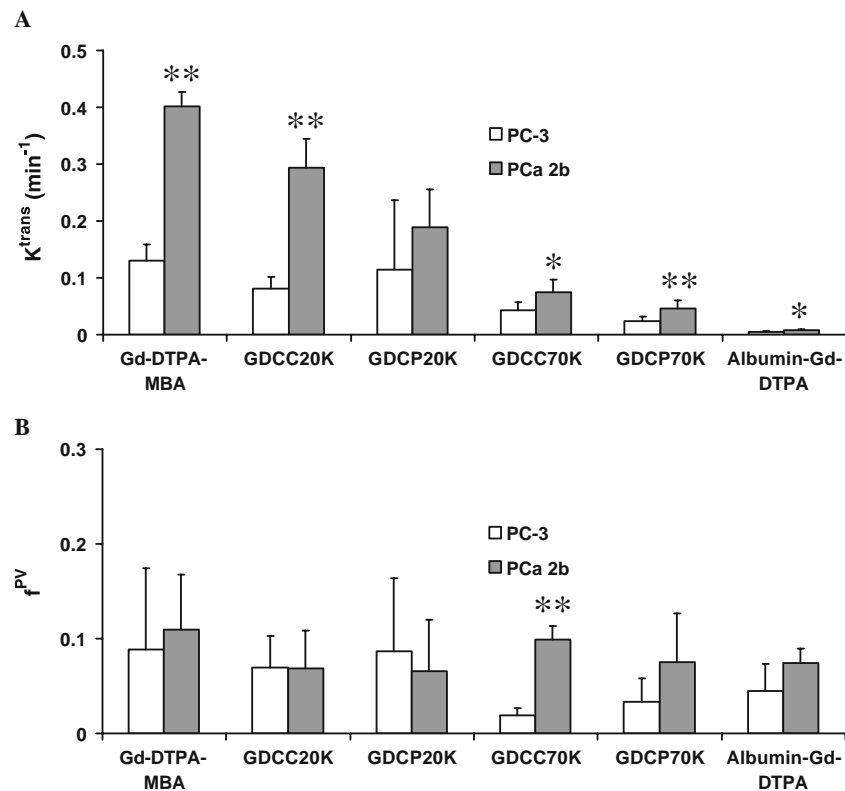


**Fig. 2.** Comparison of vascular parameters of PC-3 and MDA PCa 2b tumor xenografts estimated by Gd(DTPA-BMA), GDCC-20, GDCC-70, GDCC-20, GDCC-70, GDCC-70 and Albumin-(Gd-DTPA), respectively:  $K^{trans}$  (A) and  $f^{PV}$  (B). \* ( $P<0.05$ ), \*\* ( $P<0.01$ ).

In this study, the effectiveness of different biodegradable macromolecular MRI contrast agents in tumor characterization with DCE-MRI was preliminarily investigated in two different mouse tumor models. The results obtained with the biodegradable macromolecular contrast agents were compared to those obtained with a clinical contrast agent, Gd (DTPA-BMA), and a prototype macromolecular contrast agent, albumin-(Gd-DTPA). In both tumor models, the values of the calculated vascular parameters, particularly microvascular permeability  $K^{\text{trans}}$ , showed a dependence on size and degradability of the contrast agents (Fig. 2A). The values estimated by biodegradable macromolecular contrast agents were between those by the small molecular weight contrast agent and those by the non-degradable macromolecular contrast agent. With the same high molecular weight, GDCC-70 resulted in a higher  $K^{\text{trans}}$  values than GDCP-70 in both tumors due to high degradability of the former. However, the difference of biodegradability between GDCC-20 and GDCP-20, which had similar low molecular weight, had no significant effect on the  $K^{\text{trans}}$  values possibly due to their relatively small size and high diffusion rate from plasma to tumor extracellular space.

It appears that  $K^{\text{trans}}$  was a more sensitive parameter than  $f^{\text{PV}}$  in tumor characterization as shown in Fig. 2. There was a significant difference in  $K^{\text{trans}}$  between PC-3 and MDA PCa 2b prostate tumor xenografts estimated by most of the tested contrast agents, including Gd(DTPA-MBA), GDCC-20, GDCC-70, GDCP-70, and albumin-(Gd-DTPA). No significant difference was observed in  $K^{\text{trans}}$  between the two tumor models when assessed by GDCP-20, probably due to a relatively small sample size and large experimental errors among the samples (Fig. 1C). In contrast, the difference of  $f^{\text{PV}}$  between two tumor models was not significant for most agents except for GDCC-70. The result was consistent to the histological observation that the microvessel density was not significantly different between two tumor models. No clear trend was observed on the influence of the size and degradability of the contrast agents on the  $f^{\text{PV}}$  values.

The correlation of the  $K^{\text{trans}}$  values to physiology and histology of the tumor models is not clear. Although the MDA PCa 2b tumor xenografts grew slower than the PC-3 tumor xenografts, the  $K^{\text{trans}}$  values of the MDA PCa 2b tumor xenografts were significantly larger than those of the PC-3 tumor xenografts estimated with most of the agents. Similar uptake kinetics were reported previously by Kim *et al.* for these two tumor models with different agents (31,32). PC-3 cells are androgen-independent and poorly differentiated cells, while MDA PCa 2b cells are androgen-sensitive and relatively well-differentiated cells (38). There might be an association of tumor vascular permeability with the androgen sensitivity of the cancer. We also observed the MDA PCa 2b tumor xenografts were softer than the PC-3 tumor xenografts when palpated. Further studies are needed to understand the correlation of the  $K^{\text{trans}}$  values of the tumor models to their physiology and histology.

The degradation of the biodegradable macromolecular contrast agents might affect accurate data analysis and calculation of vascular parameters due to the change of the relaxivities of the degradation products, since the contrast agents degraded into smaller chelates during the process of the DCE-MRI data acquisition. As shown in Table I, the difference in the  $T_1$  relaxivities of biodegradable macromo-

lecular contrast agents of two different molecular weights (20 and 70 KDa) was relatively small and may not be significant in DCE-MRI data analysis because DCE-MRI is not a perfectly quantitative method. The vascular parameters calculated from the DCE-MRI data with the biodegradable macromolecular contrast agents, particularly those with a relatively large size and slow degradation rate, were comparable to those estimated by albumin-(Gd-DTPA) in both tumors without consideration of the change of relaxivities. The biodegradable macromolecular MRI contrast agents were effective in tumor characterization with DCE-MRI.

## CONCLUSIONS

Polydisulfide-based biodegradable macromolecular contrast agents' molecular weights are effective for evaluation of tumor angiogenesis with DCE-MRI using parameters such as  $f^{\text{PV}}$  and  $K^{\text{trans}}$ . These parameters are also effective to differentiate different tumor models with  $K^{\text{trans}}$  as a more sensitive parameter than  $f^{\text{PV}}$ .

## ACKNOWLEDGEMENTS

The authors thank Dr. Yong-En Sun for his technique in the tail vein catheterization and Melody Johnson for the operation of MRI scanner. This work is supported in part by the NIH grant R01 EB000489.

## REFERENCES

1. Jemal A, Siegel R, Ward E, Hao Y, Xu J, Murray T, Thun MJ. Cancer statistics. *CA Cancer J Clin.* 2008;58:71–96
2. Gossmann A, Okuhata Y, Shames DM, *et al.* Prostate cancer tumor grade differentiation with dynamic contrast-enhanced MR imaging in the rat: comparison of macromolecular and small-molecular contrast media-preliminary experience. *Radiology.* 1999;213:265–72.
3. Quinlan DM, Partin AW, Walsh PC. Can aggressive prostatic carcinomas be identified and can their natural history be altered by treatment? *Urology.* 1995;46:77–82.
4. Yancopoulos GD, Davis S, Gale NW, Rudge JS, Wiegand SJ, Holash J. Vascular-specific growth factors and blood vessel formation. *Nature.* 2000;407:242–8.
5. Ferrara N. VEGF and the quest for tumour angiogenesis factors. *Nat Rev Cancer.* 2002;2:795–803.
6. Weidner N, Semple JP, Welch WR, Folkman J. Tumor angiogenesis and metastasis-correlation in invasive breast carcinoma. *N Engl J Med.* 1991;324:1–8.
7. Aref M, Chaudhari AR, Bailey KL, Aref S, Wiener EC. Comparison of tumor histology to dynamic contrast enhanced magnetic resonance imaging-based physiological estimates. *Magn Reson Imaging.* 2008;26:1279–93.
8. Su MY, *et al.* Correlation of dynamic contrast enhanced MRI parameters with microvessel density and VEGF for assessment of angiogenesis in breast cancer. *J Magn Reson Imaging.* 2003;18:467–77.
9. Fujimoto K, *et al.* Small peripheral pulmonary carcinomas evaluated with dynamic MR imaging: correlation with tumor vascularity and prognosis. *Radiology.* 2003;227:786–93.
10. Raatschen HJ, Simon GH, Fu Y, Sennino B, Shames DM, Wendland MF, *et al.* Vascular permeability during antiangiogenesis treatment: MR imaging assay Results as biomarker for subsequent tumor growth in rats. *Radiology.* 2008;247:391–9.
11. Daldrup H, Shames DM, Wendland M, *et al.* Correlation of dynamic contrast-enhanced MR imaging with histologic tumor

- grade: comparison of macromolecular and small-molecular contrast media. *AJR Am J Roentgenol.* 1998;171:941–9.
12. Tofts PS, Brix G, Buckley DL, *et al.* Estimating kinetic parameters from dynamic contrast-enhanced T(1)-weighted MRI of a diffusable tracer: standardized quantities and symbols. *J Magn Reson Imaging.* 1999;10:223–32.
  13. Jordan BF, Runquist M, Raghunand N, *et al.* The thioredoxin-1 inhibitor 1-methylpropyl 2-imidazolyl disulfide (PX-12) decreases vascular permeability in tumor xenografts monitored by dynamic contrast enhanced magnetic resonance imaging. *Clin Cancer Res.* 2005;11:529–36.
  14. Padhani AR. Dynamic contrast-enhanced MRI in clinical oncology: current status and future directions. *J Magn Reson Imaging.* 2002;16:407–22.
  15. Roberts TP, Turetschek K, Preda A, *et al.* Tumor microvascular changes to anti-angiogenic treatment assessed by MR contrast media of different molecular weights. *Acad Radiol.* 2002;9:S511–3.
  16. Brasch RC. New directions in the development of MR imaging contrast media. *Radiology.* 1992;183:1–11.
  17. van Dijke CF, Brasch RC, Roberts TP, *et al.* Mammary carcinoma model: correlation of macromolecular contrast-enhanced MR imaging characterizations of tumor microvasculature and histologic capillary density. *Radiology.* 1996;198:813–8.
  18. de Lussanet QG, Langereis S, Beets-Tan RG, *et al.* Dynamic contrast-enhanced MR imaging kinetic parameters and molecular weight of dendritic contrast agents in tumor angiogenesis in mice. *Radiology.* 2005;235:65–72.
  19. Desser TS, Rubin DL, Muller HH, *et al.* Dynamics of tumor imaging with Gd-DTPA-polyethylene glycol polymers: dependence on molecular weight. *J Magn Reson Imaging.* 1994;4:467–72.
  20. Bogdanov AA Jr, Weissleder R, Frank HW, *et al.* A new macromolecule as a contrast agent for MR angiography: preparation, properties, and animal studies. *Radiology.* 1993;187:701–6.
  21. Su MY, Wang Z, Carpenter PM, Lao X, Muhler A, Nalcioglu O. Characterization of N-ethyl-N-nitrosourea-induced malignant and benign breast tumors in rats by using three MR contrast agents. *J. Magn. Reson. Imaging.* 1999;9:177–86.
  22. Su MY, Muhler A, Lao X, Nalcioglu O. Tumor characterization with dynamic contrast-enhanced MRI using MR contrast agents of various molecular weights. *Magn Reson Med.* 1998;39:259–69.
  23. Feng Y, Zong Y, Ke T, Jeong EK, Parker DL, Lu ZR. Pharmacokinetics, biodistribution and contrast enhanced MR blood pool imaging of Gd-DTPA cystine copolymers and Gd-DTPA cystine diethyl ester copolymers in a rat model. *Pharm Res.* 2006;23:1736–42.
  24. Preda A, van Vliet M, Krestin GP, Brasch RC, van Dijke CF. Magnetic resonance macromolecular agents for monitoring tumor microvessels and angiogenesis inhibition. *Invest Radiol.* 2006;41:325–31.
  25. Lu ZR, Parker DL, Goodrich KC, Wang X, Dalle JG, Buswell HR. Extracellular biodegradable macromolecular gadolinium (III) complexes for MRI. *Magn Reson Med.* 2004;51:27–34.
  26. Zong Y, Wang X, Goodrich KC, Mohs AM, Parker DL, Lu ZR. Contrast-enhanced MRI with new biodegradable macromolecular Gd(III) complexes in tumor-bearing mice. *Magn Reson Med.* 2005;53:835–42.
  27. Wang X, Feng Y, Ke T, Schabel M, Lu ZR. Pharmacokinetics and tissue retention of (Gd-DTPA)-cystamine copolymers, a biodegradable macromolecular magnetic resonance imaging contrast agent. *Pharm Res.* 2005;22:596–602.
  28. Feng Y, Jeong E-K, Mohs A, Emerson L, Lu Z-R. Characterization of tumor angiogenesis with dynamic contrast enhanced magnetic resonance imaging and biodegradable macromolecular contrast agents in mice. *Magn Reson Med.* 2008;60:1347–52.
  29. Ogan MD, Schmiedl U, Moseley ME, Grodd W, Paaajanen H, Brasch RC. Albumin labeled with Gd-DTPA. An intravascular contrast-enhancing agent for magnetic resonance blood pool imaging: preparation and characterization. *Invest Radiol.* 1987;22:665–71.
  30. Navone NM, Olive M, Ozen M, *et al.* Establishment of two human prostate cancer cell lines derived from a single bone metastasis. *Clin Cancer Res.* 1997;3:2493–500.
  31. Kim YR, Savellano MD, Savellano DH, Weissleder R, Bogdanov A Jr. Measurement of tumor interstitial volume fraction: method and implication for drug delivery. *Magn Reson Med.* 2004;52:485–94.
  32. Kim YR, Savellano MD, Weissleder R, Bogdanov A Jr. Steady-state and dynamic contrast MR imaging of human prostate cancer xenograft tumors: a comparative study. *Technol Cancer Res Treat.* 2002;1:489–95.
  33. Kaighn ME, Narayan KS, Ohnuki Y, Lechner JF, Jones LW. Establishment and characterization of a human prostatic carcinoma cell line (PC-3). *Invest Urol.* 1979;17:16–23.
  34. Plonowski A, Nagy A, Schally AV, Sun B, Groot K, Halmos G. *In vivo* inhibition of PC-3 human androgen-independent prostate cancer by a targeted cytotoxic bombesin analogue, AN-215. *Int J Cancer.* 2000;88:652–7.
  35. Shames DM, Kuwatsuru R, Vexler V, Muhler A, Brasch RC. Measurement of capillary permeability to macromolecules by dynamic magnetic resonance imaging: a quantitative noninvasive technique. *Magn Reson Med.* 1993;29:616–22.
  36. Weidner N, Semple JP, Welch WR, Folkman J. Tumor angiogenesis and metastasis—correlation in invasive breast carcinoma. *N Engl J Med.* 1991;324:1–8.
  37. Kobayashi H, Reijnders K, English S, Yordanov AT, Milenic DE, Sowers AL, *et al.* Application of a macromolecular contrast agent for detection of alterations of tumor vessel permeability induced by radiation. *Clin Cancer Res.* 2004;10:7712–20.
  38. Navone NM, Logothetis CJ, von Eschenbach AC, Troncoso P. Model systems of prostate cancer: uses and limitations. *Cancer Metastasis Rev.* 1999;17:361–71.